# Computational Study of Thermal Transport in Nanowire-Graphene Thin Films

Man Prakash Gupta, Nitish Kumar, and Satish Kumar

***Abstract*—Metal nanowires-doped polycrystalline graphene is recently shown to be very promising as transparent conducting material for many applications including solar cells, touchscreens, and light-emitting diodes. However, the thermal reliability of these thin-film materials can be a concern and is not well understood yet. In this study, we develop and utilize a coupled electrothermal model to examine self-heating in the nanowire-polygraphene thin-film hybrid material. We study the effects of various key material/topological parameters such as nanowire density and alignment, and interfacial thermal resistances at nanowire junctions, and nanowire-graphene interfaces on the temperature distribution of both nanowire network and polygraphene. The analysis provides useful insights about the size, location, and number of hotspots in the nanowires and polygraphene. The peak and average temperature variation in the thin-film material are explored and analyzed for varied nanowire density and percentage of high-resistance grain boundaries, and, in this respect, we observe that the variation of both peak and average temperature of the nanowire network deviates from the classical behavior expected from an electrical conductor, and rather it follows the trend according to the copercolating charge transport within the nanowire-polygraphene hybrid material. We find that the temperature profile of nanowires follows the Weibull distribution for various current values in the network for both below and above percolation threshold of nanowire networks. We systematically study the effect of nanowire orientation on the temperature profile in the material, and find that aligned nanowires along the main transport direction is likely to experience higher temperature rise due to the enhanced current. The developed framework can help us to provide design guidelines to mitigate the bottlenecks and accelerate the advent of these types of hybrid materials as transparent conducting electrodes.**

***Index Terms*—Thermal transport, Nanowire-Graphene, Percolation, Electro-thermal model, Computational, Grain boundary.**

## I. Introduction

TRANSPARENT conducting materials (TCMs) are utilized in many applications including solar cells, touch-screens, displays, photodetectors, and organic light-emitting diodes [1], [2]. Significant research efforts are underway to find new materials which can replace the commonly used but increasingly expensive Indium Tin Oxide as TCM [3]–[10]. Single-layer graphene have been shown to have excellent electrical conductivity and very high optical transmittance which are desired properties for TCMs [11], [12]. However, the chemical vapor deposition grown large area graphene is polycrystalline, and their electrical conductivity is greatly reduced due to the scattering of charge carriers from various defects. Recent studies have reported that the transport properties of polygraphene can be significantly improved (sheet resistivity $<20\ \Omega$/sq; transparency $>90\%$ for visible light) by the addition of silver nanowires on polygraphene [13], [14]. Metallic nanowires provide low resistance percolating pathways over the defects such as the grain boundaries which increases the overall conductance of the thin-film material.

It should also be noted that silver nanowires themselves are considered to be potential candidates for transparent conducting electrodes (TCEs). However, the high electrical resistance at the nanowire junctions reduces the overall conductance of nanowires network making them less appealing as TCEs. Some techniques such as plasmon-induced chemical reaction [15], electric-field assisted spray coating [16], light-induced plasmonic nano-welding [17], and nano-welding using localized Joule heating [18] have been used to improve the junction resistance. However, concerns still remain since the silver nanowires are highly susceptible to the excessive Joule heating. Khaligh *et al.* [19] studied the reliability aspects of silver nanowires under electrical current flow for organic solar cell applications. They found that silver nanowires network based electrodes get significantly damaged within a couple of days due to excessive Joule heating. Chen *et al.* [20] found that silver nanowire network becomes unusable for optoelectronic devices due to decreased conductivity, transparency and fragmentation of nanowires at current density of $150\,\text{mA/cm}^2$. Given the susceptibility of Silver nanowires to material degradation from excessive heat dissipation, examination of self-heating in nanowire-doped polygraphene hybrid materials becomes very important since these thin-film materials are deposited on low-thermal conductivity substrates. Only a handful of studies have been performed to study the thermal behavior of nanowire-polygraphene hybrid thin-film material under electrical current flow [21], [22]. Maize *et al.* [22] performed temperature measurement of nanowire-polygraphene thin-film using thermoreflectance technique. They compared the temperature of Silver nanowires with and without graphene, and found that graphene's

Manuscript received January 17, 2018; revised May 1, 2018; accepted May 26, 2018. Date of publication June 4, 2018; date of current version July 9, 2018. The review of this paper was arranged by Associate Editor H. Zhang. *(Corresponding author: Nitish Kumar.)*

M. P. Gupta was with the G. W. W. School of Mechanical Engineering, Georgia Institute of Technology, Atlanta, GA 30332 USA. He is now with Ford Motor Company, Dearborn, MI 48126 USA (e-mail: manprakashg@gmail.com).

N. Kumar and S. Kumar are with the G. W. W. School of Mechanical Engineering, Georgia Institute of Technology, Atlanta, GA 30332 USA (e-mail: nitish.kumar@gatech.edu; satish.kumar@me.gatech.edu).

This paper has supplementary downloadable material available at http://ieeexplore.ieee.org.

Digital Object Identifier 10.1109/TNANO.2018.2843386

presence lowers the temperature of nanowires due to enhanced heat transfer by graphene. Das *et al.* [21] presented a statistical analysis of the temperature profile of nanowire/graphene thin-film composites, obtained from the thermoreflectance imaging technique. They found that the temperature distribution of nanowires follows Weibull distribution above the percolation threshold but distribution in other regimes, e.g., below percolation threshold is still unknown. These studies suggest that the combination of nanowires and polygraphene is mutually beneficial to both nanowires and polygraphene. Nanowires and polygraphene provide low resistance pathways for each other at their electrically challenged places (junctions in case of nanowires, and grain boundary defects for polygraphene). Additionally, polygraphene can help provide efficient heat-transfer pathways for the nanowires. Thermoreflectance imaging has limit on the spatial resolution and the previous studies could not resolve the temperature distribution along nanowires or along polygraphene. Computational modeling of electro-thermal transport in these materials can be very helpful in this regard, and can provide useful insights into the long-term thermal stability and reliability improvements. To the best of our knowledge, there has been no prior study regarding the electro-thermal transport modeling in nanowire-polygraphene composites.

It is to be noted here that obtaining the simultaneous information about electro-thermal transport variables (e.g., the current, potential, heat dissipation, and temperature) with nanometer resolution remains a challenging task for experimental tools and techniques. Mesoscale modeling and simulations of materials and devices are extremely useful in overcoming these challenges as they can provide detailed information about these transport variables at hierarchical length scales, are relatively much inexpensive and less time-consuming. Furthermore, the computational analysis of these variables can provide important insights into the material/ device performance bottlenecks. These insights can also be used to find innovative solutions to design the material processing steps to optimize the material properties for specific applications such as solar cells, displays, and light-emitting diodes. The objectives of the current study are: (1) to obtain and examine the quantitative information about both the heat and charge transport variables simultaneously in hybrid structures containing nanowires dispersed on polycrystalline graphene, (2) to compare the electrical and thermal behavior of such composites or thin films with their individual constituents, i.e., nanowire network and polycrystalline graphene, (3) to investigate the factors associated with the excessive Joule heating which can affect the operational reliability of such composite materials (under what conditions nanowire is likely to fail, the role of junctions and dynamics of current crowding, investigation of self-heating), (4) to examine the role of nanowire junctions in the current and temperature distribution, (5) to develop a framework which can provide useful design guidelines to mitigate the bottlenecks and accelerate the advent of these materials as TCEs.

## II. Methodology

We develop a computational method to investigate the thermal transport in the composite; this coupled electro-thermal model is described below. The shape of single crystal domains (referred to as 'grains') in polycrystalline graphene is typically non-uniform with stochastic variation [23], [24]. However, it has been reported that on average, sheet conductance of polygraphene is nearly independent of the grain-shape [13]. Therefore, we assume square grains for the computational model developed to analyze polygraphene (Fig. 1). The grain size (4 $\mu$m) and nanowires length (10 $\mu$m) considered in the present study, are sufficiently larger than the mean free path of charge carriers, and therefore charge transport can aptly be described by diffusive transport theory. This approximation has been validated and successfully applied for the carbon nanotube network based devices previously [25]–[27].

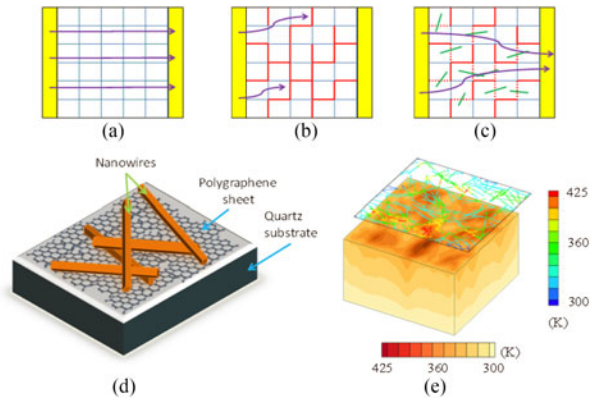


Fig. 1. (a)–(c) Schematic depicts how the presence of nanowires on polygraphene may enhance the both the charge and heat transport. Here, yellow region represents the electrodes, thin blue and thick red lines represent the low and high resistance grain boundaries (assuming square crystal domains). (d) Schematic of nanowire-dispersed polygraphene thin-film on quartz substrate. (e) Temperature profile of nanowire network and polygraphene on quartz substrate obtained from the numerical model.

We consider the grain boundary resistance value to be of binary nature, i.e., it is either low (same value as that of the intra-grain resistance) or high (60 times the value of intra-grain resistance) similar to previous studies [13], [28]. We randomly selected the location of the high resistance grain boundaries (Fig. 1). The length of the nanowire is considered to be 10 $\mu$m and the diameter is 100 nm. Nanowires are randomly oriented unless specified otherwise with nominal density of the nanowire network as $6 \times 10^4$ nanowires/mm$^2$. Statistical averaging is performed over more than 100 ensembles of nanowire-polygraphene films wherever needed for data analysis.

### A. Electric Transport

Governing equations are based on the charge conservation principle utilizing the diffusive transport theory. Equation (1) and (2) describe the charge transport in the ensemble of 1-D nanowires and 2-D polygraphene sheet respectively, and they also include the interaction among the nanowires at the junctions, and between nanowires and polygraphene.

$$\frac{d^2\psi_i}{ds^{*2}} + \tilde{G}_C\left(\psi_g - \psi_i\right) + \sum_{\substack{\text{intersecting} \\ \text{NWs j}}} \tilde{G}_{Jun}\left(\psi_j - \psi_i\right) = 0 \quad (1)$$

$$\nabla^{*2}\psi_g + \sum_{i=1}^{N_{\text{tubes}}} \tilde{G}_C \beta_v \left(\psi_i - \psi_g\right) = 0 \tag{2}$$

Here, $\Psi$ denotes the electric potential. All lengths are non-dimensionalized by the nanowire diameter (*d*). $\Psi_i$ and $\Psi_g$ denote the local potentials of a nanowire and polygraphene respectively. The second and third terms in (1) represent the charge transfer between nanowire and polygraphene, and at the nanowire junctions respectively. $\tilde{G}_C$ and $\tilde{G}_{Jun}$ are non-dimensional contact conductance at nanowire-to-graphene and nanowire-to-nanowire contacts respectively, defined as follows [26], [29]:

$$\tilde{G}_C = \frac{g_C P_C d^2}{\sigma_{NW} A}; \quad \tilde{G}_{Jun} = \frac{g_{Jun} P_{Jun} d^2}{\sigma_{NW} A};$$
$$\beta_v = \alpha_v \left(\frac{A}{P_S}\right) \frac{\sigma_{NW}}{\sigma_{Graphene}}$$

Here, $g_C$ and $g_{Jun}$ are contact conductances per unit area at nanowire-to-graphene and nanowire-to-nanowire contacts respectively; $P_C$ and $P_{Jun}$ are the corresponding contact perimeters. $\sigma_{NW}$ and $\sigma_{Graphene}$ are the electrical conductivity of nanowire and graphene, respectively. *A* is the cross-sectional area of the nanowire. The parameter $\beta_v$ characterizes the contact geometry and $\alpha_v$ is the contact area per unit volume (area $\times$ thickness) of graphene cell. The intra-grain electrical resistance of polygraphene is taken to be 30 Ω/sq assuming only the acoustic deformation potential scattering [30]. The nanowire electrical resistivity is taken as $2 \times 10^{-8}$ Ω–m, consistent with the values reported in the literature [31]. The contact resistance between nanowire and graphene is considered to be 200 Ω – $\mu$m [13]. The resistance at the nanowire junctions is taken as 10 Ω [31]. The boundaries at $x = 0$, and $x = L_x$, are kept at 1 V and 0 V, respectively. Boundaries at $y = 0$, $y = L_y$ are considered to be periodic.

### *B. Thermal Transport*

Governing equations are based on the energy conservation principle utilizing the diffusive transport theory. Equations (3), (4), and (5) describe the thermal transport in the ensemble of 1-D nanowires, the 2-D polygraphene sheet, and quartz substrate respectively. Equation (3) and (4) also includes the interaction among the nanowires at the junctions, and between nanowires and polygraphene.

$$\frac{d^2\theta_i}{ds^{*2}} + Bi_C\left(\theta_g - \theta_i\right) + \sum_{\substack{\text{intersecting} \\ \text{NWs j}}} Bi_{Jun}\left(\theta_j - \theta_i\right) + \frac{d}{L_{NW}}\frac{\dot{Q}}{\dot{Q}_{ref}} = 0 \tag{3}$$

$$\nabla^{*2}\theta_g + \sum_{i=1}^{N_{\text{tubes}}} Bi_C \gamma_v \left(\theta_i - \theta_g\right) = 0 \tag{4}$$

$$\nabla^{*2}\theta_{Sub} = 0 \tag{5}$$

Here, temperature (*T*) is non-dimensionlized as $\theta = (\mathrm{T} - \mathrm{T}_\infty)/(\mathrm{Q'}_{\mathrm{ref}} d L_{\mathrm{NW}} k_{\mathrm{NW}})$. All lengths are non-dimensionalized by the nanowire diameter (*d*). $\dot{Q}(= \overrightarrow{J} \bullet \overrightarrow{E}$ , here $\overrightarrow{J}$ is current density and $\overrightarrow{E}$ is electric field) is the Joule heating term and $\dot{Q}_{ref}$ is the reference power density. $\theta_i$, $\theta_g$, and $\theta_{Sub}$ denote the local temperatures of $i$th section of a nanowire, polygraphene, and the quartz substrate respectively. The second and third term in (1) represent the thermal interaction between nanowire and polygraphene, and at the nanowire junctions respectively. $Bi_C$ and $Bi_{Jun}$ are non-dimensional thermal contact conductance at nanowire-to-graphene and nanowire-to-nanowire contacts respectively, defined as follows [26], [29]:

$$Bi_C = \frac{h_C P_C d^2}{k_{NW} A}; \quad Bi_{Jun} = \frac{h_{Jun} P_{Jun} d^2}{k_{NW} A};$$
$$\gamma_v = \alpha_v \left(\frac{A}{P_S}\right) \frac{k_{NW}}{k_{Graphene}}$$

Here, $h_C$ and $h_{Jun}$ are thermal contact conductances per unit area at nanowire-to-graphene and nanowire-to-nanowire contacts respectively; $P_C$ and $P_{Jun}$ are the corresponding contact perimeters. $k_{NW}$ and $k_{Graphene}$ are the thermal conductivity of nanowire and graphene. *A* is the cross-sectional area of nanowire. The parameter $\gamma_v$ characterizes the contact geometry and $\alpha_v$ is the contact area per unit volume (area $\times$ thickness) of graphene cell. Polygraphene sheet is considered to be deposited on a fused quartz substrate of thickness 0.5 mm. Intra-grain thermal conductivity of the polygraphene is considered to be 600 W/mK [32]. Thermal conductivity of silver nanowire is assumed to be 200 W/mK [33]. Thermal conductivity of the fused quartz substrate is taken to be 1.4 W/mK [34]. The thermal contact resistance between quartz and polygraphene sheet is taken as $1.2 \times 10^{-8}$ $\mathrm{m}^2$ K/W [35]. Polygraphene sample size ($L_x \times L_y$) is taken to be 52 $\mu$m $\times$ 52 $\mu$m in the present study. The grain size for most of the simulation results is considered to be 4 $\mu$m, which is consistent with the values reported in literature [36]. Each grain region is discretized into $10 \times 10$ cells. Boundaries at $y = 0$, $y = L_y$ are considered to be periodic. Bottom of the quartz substrate is considered to be at 300 K. All other boundaries are treated as adiabatic.

## III. Results and Discussion

Here, we investigate the transport in the nanowire-polygraphene hybrid structure using the developed model that allows us to find insights into the plausible correlations between the topological/material properties of the hybrid structure and its electro-thermal characteristics.

The computational model allows us to obtain quantitative information about several electro-thermal transport variables such as electrostatic potential, electric current, power dissipation, and the temperature simultaneously as shown in Fig. 2. Here, 60% grain boundaries are considered to be of high resistance, and the nanowire network density is $D = 6 \times 10^4/\mathrm{mm}^2$. It can be noted that the electrical current favors low resistance pathways within the nanowire-polygraphene hybrid material. This leads to a non-uniform distribution of not only the electrical current but also the

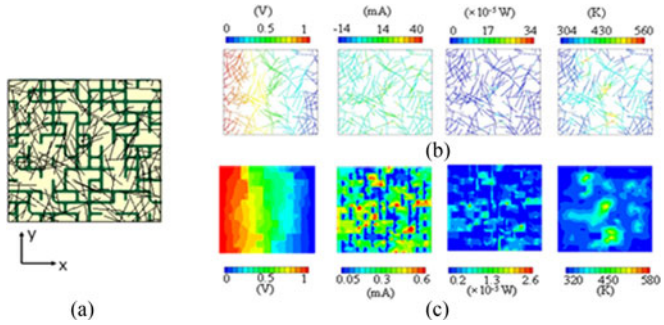


Fig. 2. (a) Schematic of nanowire dispersed polygraphene material; here, thick green lines represent the high resistance grain boundaries of polygraphene, and the black lines represent the nanowires. Contour plots of electrostatic potential (V), current (mA), Joule heating (W), and temperature (K) (in the order of left to right respectively) of the (b) nanowire network, and (c) polygraphene. Here, we consider nanowire network density $= 6 \times 10^4$ /mm$^2$ and 60% high resistance grain boundaries in polygraphene.

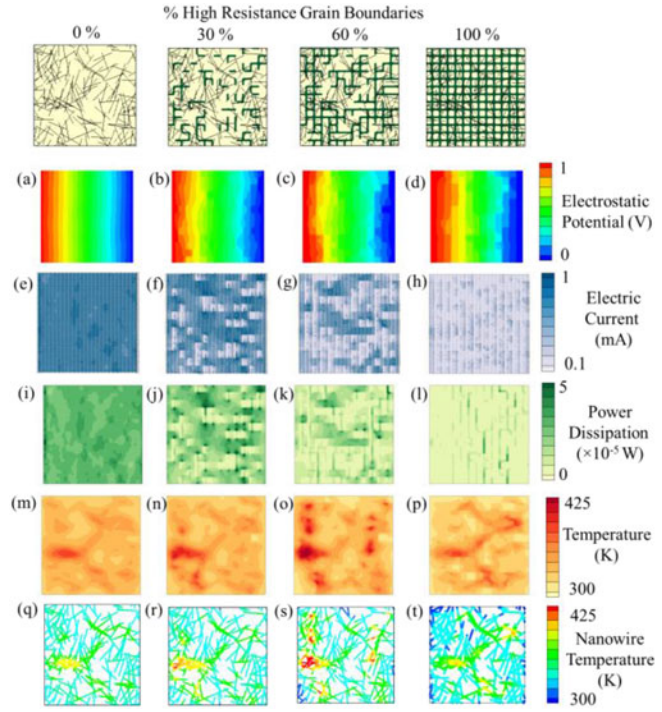


Fig. 3. (Top row) Schematic representation of nanowire-polygraphene hybrid material for 0%, 30%, 60%, and 100% (left to right, respectively) of high resistance grain boundaries. (a–t) Polygraphene contour plots of electrostatic potential (V), current (mA), Joule heating (W), temperature (K) and nanowire temperature (K) (second from top to bottom row, respectively). Nanowire network density $= 6 \times 10^4$/mm$^2$.

Joule heating and the temperature both in the nanowire network and the polygraphene (Fig. 2). The temperature hot-spots in the nanowire network is indicative of the 'current crowding' occurring at certain nanowires where they help provide critical low resistance pathways across the high resistance grain boundaries of polygraphene.

Fig. 3 shows the contour plots of electrostatic potential, electric current, power dissipation, and temperature profile in polygraphene sheet for four cases of high resistance grain boundaries (GBs): 0%, 30%, 60%, and 100% at nanowire network density, $D = 6 \times 10^4$ /mm$^2$. Although, the contour profile in these plots can vary depending on the spatial distribution of both the nanowires and the high resistance GBs, a few observations about the general trend can still be made based on these plots. The distribution of the electrostatic potential in the polygraphene seems more sensitive to the high resistance grain boundaries rather than to the nanowires (Fig. 3a–d). The electric current in the polygraphene sheet decreases with increasing % of high resistance GBs (Fig. 3e–h). The electrical current flows through the available low resistance pathways in the hybrid structure. In particular, above the percolation threshold of high resistance GBs (∼60%), nanowires play the important role in providing low resistance pathways over the high resistance GBs. This becomes very apparent in case of 100% high resistance GB case, when electric current is observed to be mainly along the footprints of nanowires on the polygraphene sheet (Fig. 3h). The distribution of Joule heating (Figures 2, and 3) in the hybrid structure is seen to be directly affected by the pathways of current flow which depends on both the density and distribution of nanowires and high resistance GBs (See Figures S1–S7 in the supplementary document for current, potential, power dissipation, and temperature–for different % of high resistance grain boundaries and density of nanowire network). The overall Joule heating decreases with the increase in the % of high resistance GBs due to the reduced current flow. Fig. 3(m–p) show the temperature profile in the polygraphene sheet. In Fig. 3, the highest temperature is observed for 60% of high resistance GBs. Again, this is a consequence of the current crowding and high power dissipation in a specific location of network which is dependent on the relative distribution of nanowires with respect to the high resistance grain-boundaries of poly-graphene (more discussion later). It is to be pointed out here that the location of hot-spots and overall temperature profile in the polygraphene sheet depends more on the spatial distribution of nanowire networks rather than the power dissipation profile of the polygraphene sheet as also seen previously in Fig. 2 and also in Figure S1–S6 in the supplementary.

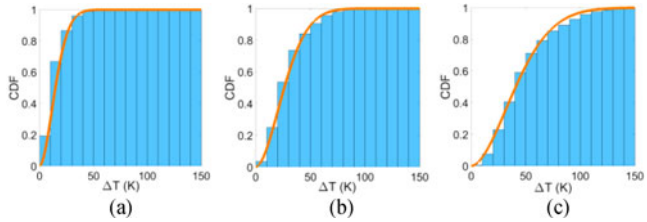


Fig. 4. Cumulative distribution function (CDF) of Weibull distribution (CDF $= 1 - \exp(-\Delta T/\lambda)^k$) for the temperature distribution corresponding to three different currents: (a) I $= 12$ mA, (a) I $= 16$ mA, and (a) I $= 20$ mA, with scale parameter, $\lambda = 18$ K, 32 K, and 50 K for three cases respectively. Shape parameter, $k = 1.8$ for all cases.

Fig. 4 shows the cumulative distribution function of the temperature profile of nanowire network. We observed that the temperature profile of nanowires follows the Weibull distribution for various current values in the network. CDF $= 1 - \exp(-\Delta T/\lambda)^k$. The shape parameter, $\lambda$ of the Weibull distribution follows the square law with respect to the cur-

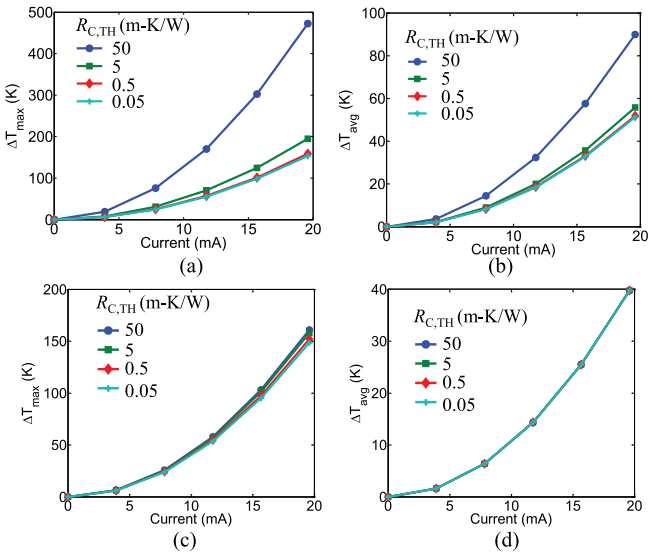


Fig. 5. Effect of increasing current in the nanowire-polygraphene thin-film on the temperature. The maximum and average temperature in (a, b) nanowire network and (c, d) polygraphene. $R_{C,TH}$ is the contact resistance between nanowires and polygraphene sheet. (a, b) correspond to nanowires, and (c, d) correspond to polygraphene.

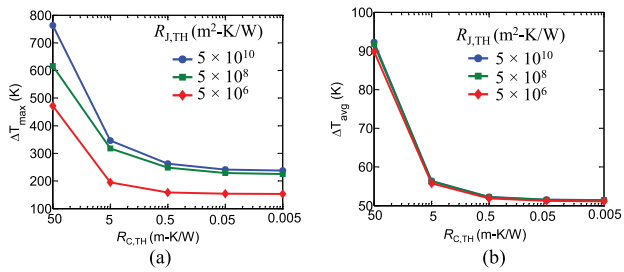


Fig. 6. Effect of thermal contact resistance at nanowire junctions on the temperature. The change in (a) maximum temperature, (b) average temperature in nanowires network is shown. $R_{J,TH}$ is the contact thermal resistance at nanowire junctions.

rent such that $\lambda = \alpha I^2$. These results are consistent with the experimental results [21], and therefore, imply the validity of the current modeling approach. Fig. 5 shows the variation of the peak and average temperature in polygraphene and nanowire networks. Since the electro-thermal model is linear in nature, square Ohmic law ($\Delta T \sim P_{diss} \sim I^2$) is observed to be followed by peak and average temperature of both nanowires and polygraphene with respect to the variation in current irrespective of the value of nanowire-graphene contact resistance.

Fig. 6 shows the peak and average temperature rise in nanowires for varied thermal contact resistance at nanowire junctions ($R_{J,TH}$), and graphene-nanowire interface ($R_{C,TH}$). The values of these resistances are chosen in such a way that they represent full range of the quality of thermal contacts from poor to extremely good. For a given thermal contact resistance at the nanowire junctions, the maximum and average temperature both decrease with decreasing contact resistance between the

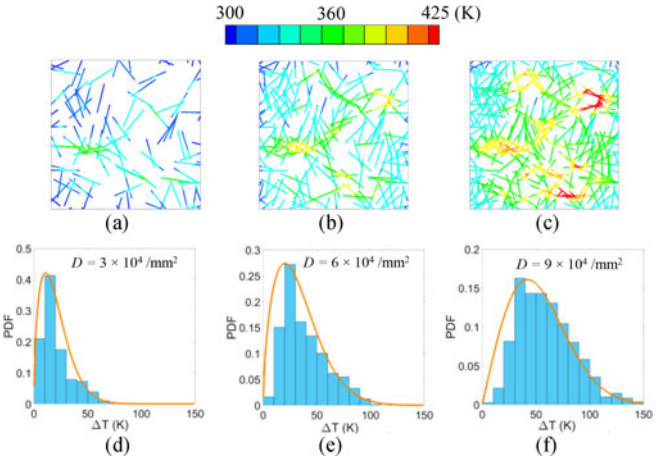


Fig. 7. Temperature distribution of nanowires corresponding to three different nanowire network densities, $D = 3 \times 10^4$/mm$^2$, $6 \times 10^4$/mm$^2$, and $9 \times 10^4$/mm$^2$ (from left to right, respectively). Top row shows the temperature profile in the nanowires, (b) bottom row provide the statistical information about the temperature variation in the nanowires, and it shows that temperature follows the PDF of the Weibull distribution both below and above percolation threshold of the nanowire networks.

nanowires and graphene. The temperature decreases sharply as $R_{C,TH}$ decreases from 50 to 5 m-K/W, but changes very little when $R_{C,TH}$ is reduced after 0.5 m-K/W. This suggests that 0.5 m-K/W corresponds to an excellent thermal contact between nanowires and graphene. We find that the thermal contact resistance between nanowires and graphene ($R_{C,TH}$) significantly affects the temperature of the nanowires; good thermal contact between nanowires and polygraphene are necessary to efficiently dissipate the heat away from the nanowires as observed in the experiments [22]. The peak temperature of nanowires decreases significantly when junction resistance is lowered, however the average temperature remains almost invariant with respect to the junction resistance. This implies that the number and size of hotspots are relatively very small, and the thermal interaction among nanowires plays important role in reducing the temperature at these hot-spots. Detailed contour plots are provided in the supplementary material which provide more information about the hot-spots as a function of nanowire density and % high resistance grain boundaries (see Figs. S1–S6). As mentioned earlier, hot-spots are likely to appear at those nanowires which play critical role in providing percolative current pathways, and junctions at these nanowires are likely to be more susceptible to very high temperature increase, which may lead to thermal-transpired cracks or even local melting. This may lead to re-routing of the current pathways, and may lead to more such events at other nanowires subsequently. The rise in the temperature may lead to electromigration of Silver [16], [22]. The welding of nanowires at the junctions reduces the electrical contact resistance, and therefore enhances the overall conductance of the nanowire network. By improving the junction resistance, the hot-spot temperature can be lowered significantly, which can effectively improve the material life span under extreme electro-thermal load or Joule heating.

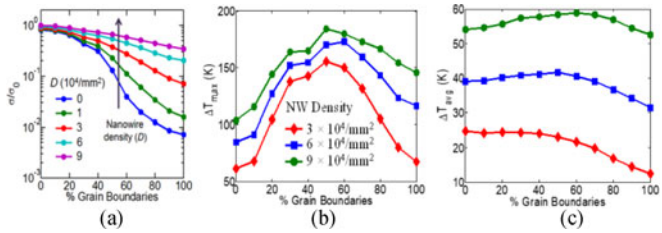


Fig. 8. Effect of variation in percentage high resistance grain boundaries on (a) normalized electrical conductance, (b) peak temperature and (c) average temperature of nanowires-polygraphene at different nanowire densities.

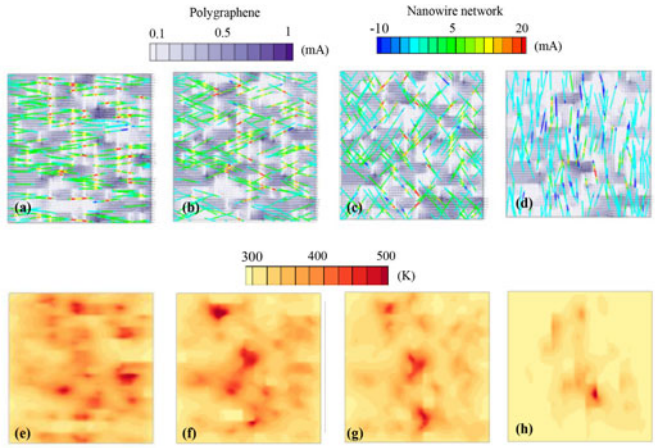


Fig. 9. (Top row) Contour profiles of electric current flow in the nanowire network and polygraphene sheet for four different alignment angles 0°, 30°, 60°, and 80° (left to right, respectively). Red segments in the nanowires can be noted over the high resistance grain boundaries indicating higher current flow in the nanowires at these locations. (Bottom row) shows the temperature profile in the polygraphene sheet corresponding to four alignment cases shown above.

Fig. 7 shows the temperature profile of nanowire network for three different network densities: $3 \times 10^4/\text{mm}^2$, $6 \times 10^4/\text{mm}^2$, and $9 \times 10^4/\text{mm}^2$. We find that the temperature profile of nanowires follows Weibull distribution which is also suggested by the previous experimental studies [21]. The shape and scaling parameters of the distribution depend on the nanowire density. However, the Weibull distribution remains applicable for both below and above percolation threshold density of the nanowires. This finding emphasizes that the developed model can be used in exploring the unique and novel properties of hybrid materials like nanowires-graphene considering the statistical distribution of the network. We find that for $D = 3 \times 10^4/\text{mm}^2$, temperature rise remains between 0 and 50 K, with maximum number of nanowires maintaining a temperature rise of 10 K. As the density of nanowires increases, the spread of temperature rise also increases to range of 0 – 100 K and 0 – 150 K corresponding to $D = 6 \times 10^4/\text{mm}^2$ and $D = 9 \times 10^4/\text{mm}^2$ respectively. It should be noted that the location of the hot-spot not only depends on density and distribution of nanowires but also on the location of grain boundaries. Usually, the nanowires which provide critical current carrying pathways in the nanowire-polygraphene composites are likely to experience larger Joule heating and consequently higher temperature rise.

Fig. 8 shows the effect of % high resistance GBs on the electrical conductance and temperature of nanowire-dispersed on polygraphene. Electrical conductance of polygraphene sheet without nanowires decreases by more than two orders of magnitude when high resistance GBs varies from 0% to 100%. Addition of nanowires increases the conductance of the material, but their effect becomes more pronounced when % of high resistance GBs is greater than the percolation threshold (∼60%) for charge transport (Fig. 8a) [28]. We note that both peak and average temperatures in the hybrid structure increase with the nanowire density at a given high resistance GBs. This is attributed to more current carrying pathways available in the materials with the increase in the number of nanowires leading to more current and hence more Joule heating. Further, we find that peak temperature reaches a maximum at 60% high resistance GBs for the given network densities. This is because the electric current in polygraphene sheet decreases substantially above 60% of high resistance GBs due to its own percolative nature of charge transport and the associated percolation threshold [28]. However, the presence of nanowires on polygraphene provides additional percolating pathways over the high resistance GBs. Moreover, near this percolation threshold some nanowires incidentally located near those GBs can open up the low resistance pathways across the polygraphene sheet. These nanowires are likely to face higher local current flow resulting in higher Joule heating and relatively very high temperature rise compared to surroundings. Such locations in the nanowires tend to show the peak temperature of the material (See Figure S7 in the supplementary document). The average temperature of the material shows a different behavior (Fig. 8c). For nanowire density, $D = 3 \times 10^4/\text{mm}^2$, we find that the average temperature remains nearly unchanged for 0% to 40% high resistance GBs, and then decreases at further increase of high resistance GBs. For nanowire density, $D = 6 \times 10^4/\text{mm}^2$ (or $9 \times 10^4/\text{mm}^2$), the average temperature increases slowly for 0% to 50% (or 60%) high resistance GBs, and then decreases with further increase of % of high resistance GBs. This variation is consistent with how the electric current varies in the hybrid structure as a function of % of high resistance GBs. The trend can be understood by a simple relation: $T_{\text{avg}}\, \alpha\, P_{\text{avg}} \sim I^2 R_{\text{total}}$, here $T_{\text{avg}}$, $P_{\text{avg}}$, $I$, $R_{\text{total}}$ are average temperature, average power dissipation, total current and total electrical resistance respectively. Increasing the number of nanowires increases the available pathways for charge transport and therefore increases the total current ($I$). So, for a given % of high resistance GBs, the increase in the nanowire density results in net increase in the current ($I$) which leads to higher power dissipation ($P_{\text{avg}}$) and greater average temperature ($T_{\text{avg}}$). Increasing the % of high resistance GBs increases the total resistance ($R_{\text{total}}$) which decreases the total current ($I$) since $I\, \alpha\, 1/R_{\text{total}}$.

We further examine the effect of nanowire alignment on the temperature of the hybrid structure. We vary the alignment angle of nanowires between 0° and 90°. Here, 0° and 90° alignment angles indicate that the nanowires are aligned parallel and perpendicular to the main carrier transport direction, respectively. Fig. 9 shows the contour plots of current flow and the temperature profile in the material. It can be noted that lesser number of

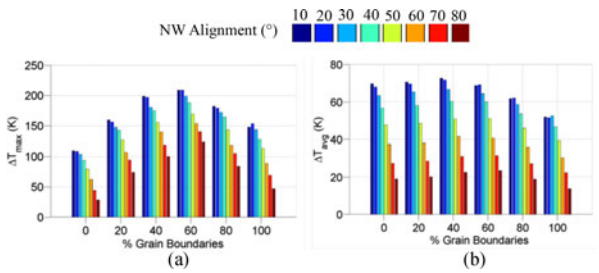


Fig. 10. Variation of peak temperature and average temperature of nanowires with different percentages of high resistance grain boundaries at varied alignment angles.

nanowires help bridge the high resistance GBs in the direction of main carrier transport when the alignment angle is increased. This leads to lower current flow and reduced power dissipation which results in lower temperature rise. Fig. 10 shows the effect of nanowire alignment on the peak and average temperature of nanowires for different % of high resistance GBs at nanowire density $(D) = 6 \times 10^4/\text{mm}^2$. We find that for a given high resistance GBs, both peak and average temperatures decrease as the alignment angle increases from 0° to 90°.

## IV. Conclusion

We develop a computational model to study the electro-thermal transport in nanowire-polygraphene thin-film composite to examine self-heating effects. The developed model allows us to obtain the fine details of the current and temperature distribution as a function of various material/topological parameters of the hybrid material. We study the thermal effects of various key parameters such as nanowire density and alignment, and interfacial thermal resistances at nanowire junctions, and nanowire-graphene interfaces. We find that the temperature profile of nanowires follows the Weibull distribution for various current values in the network for both below and above percolation threshold of nanowire networks. We observe that the variation of both peak and average temperature of the nanowire network deviates from the classical behavior and rather it follows the trend according to the co-percolating charge transport within the nanowire-polygraphene hybrid material. We also estimate the thermal contact resistances values corresponding to varying quality of thermal contacts in the material. Results suggest that 0.5 m-K/W corresponds to an excellent thermal contact between nanowires and graphene. Detailed contour plots provide useful insights about the size, location and number of hotspots in the nanowires and polygraphene. The peak and average temperature variation in the thin-film material are explored and analyzed for varied nanowire density and % of high resistance grain boundaries. We also examine the effects of nanowire orientation on the temperature profile in the material, and find that aligned nanowires along the main transport direction are likely face more Joule heating and greater temperature rise due to enhanced current. Results presented in the study provide important insights into the thermal transport behavior in the nanowire-polygraphene thin-film material which can be used to improve the thermal reliability of these materials.

## References

[1] E. F-ortunato, D. Ginley, H. Hosono, and D. C. Paine, "Transparent conducting oxides for photovoltaics," (in English), *MRS Bull.*, vol. 32, no. 3, pp. 242–247, Mar. 2007.

[2] K. Ellmer, "Past achievements and future challenges in the development of optically transparent electrodes," (in English), *Nature Photon.*, vol. 6, no. 12, pp. 808–816, Dec. 2012.

[3] D. S. Hecht, L. B. Hu, and G. Irvin, "Emerging transparent electrodes based on thin films of carbon nanotubes, graphene, and metallic nanostructures," (in English), *Adv. Mater.*, vol. 23, no. 13, pp. 1482–1513, Apr. 5, 2011.

[4] C. F. Guo *et al.*, "Fatigue-free, superstretchable, transparent, and biocompatible metal electrodes," (in English), *Proc. Nat. Acad. Sci. USA*, vol. 112, no. 40, pp. 12332–12337, Oct. 6, 2015.

[5] C. F. Guo, T. Y. Sun, Q. H. Liu, Z. G. Suo, and Z. F. Ren, "Highly stretchable and transparent nanomesh electrodes made by grain boundary lithography," (in English), *Nature Commun.*, vol. 5, Jan. 2014, Art. no. 3121.

[6] J. J. Liang, L. Li, X. F. Niu, Z. B. Yu, and Q. B. Pei, "Elastomeric polymer light-emitting devices and displays," (in English), *Nature Photon.*, vol. 7, no. 10, pp. 817–824, Oct. 2013.

[7] K. S. Kim *et al.*, "Large-scale pattern growth of graphene films for stretchable transparent electrodes," (in English), *Nature*, vol. 457, no. 7230, pp. 706–710, Feb. 5, 2009.

[8] L. Xiao *et al.*, "Flexible, stretchable, transparent carbon nanotube thin film loudspeakers," (in English), *Nano Lett.*, vol. 8, no. 12, pp. 4539–4545, Dec. 2008.

[9] L. Cai *et al.*, "Highly transparent and conductive stretchable conductors based on hierarchical reticulate single-walled carbon nanotube architecture," (in English), *Adv. Funct. Mater.*, vol. 22, no. 24, pp. 5238–5244, Dec. 19, 2012.

[10] D. J. Lipomi *et al.*, "Skin-like pressure and strain sensors based on transparent elastic films of carbon nanotubes," (in English), *Nature Nanotechnol.*, vol. 6, no. 12, pp. 788–792, Dec. 2011.

[11] R. R. Nair *et al.*, "Fine structure constant defines visual transparency of graphene," (in English), *Science*, vol. 320, no. 5881, pp. 1308–1308, Jun. 6, 2008.

[12] S. V. Morozov *et al.*, "Giant intrinsic carrier mobilities in graphene and its bilayer," (in English), *Phys. Rev.Lett.*, vol. 100, no. 1, p. 016602, Jan. 11, 2008.

[13] C. W. Jeong, P. Nair, M. Khan, M. Lundstrom, and M. A. Alam, "Prospects for nanowire-doped polycrystalline graphene films for ultratransparent, highly conductive electrodes," (in English), *Nano Lett.*, vol. 11, no. 11, pp. 5020–5025, Nov. 2011.

[14] B. Deng *et al.*, "Roll-to-Roll encapsulation of metal nanowires between graphene and plastic substrate for high-performance flexible transparent electrodes," (in English), *Nano Lett.*, vol. 15, no. 6, pp. 4206–4213, Jun. 2015.

[15] H. F. Lu, D. Zhang, X. G. Ren, J. Liu, and W. C. H. Choy, "Selective growth and integration of silver nanoparticles on silver nanowires at room conditions for transparent nano-network electrode," (in English), *ACS Nano*, vol. 8, no. 10, pp. 10980–10987, Oct. 2014.

[16] B. Seong, I. Chae, H. Lee, V. D. Nguyen, and D. Byun, "Spontaneous self-welding of silver nanowire networks," (in English), *Phys. Chem. Chem. Phys.*, vol. 17, no. 12, pp. 7629–7633, 2015.

[17] E. C. Garnett *et al.*, "Self-limited plasmonic welding of silver nanowire junctions," (in English), *Nature Mater.*, vol. 11, no. 3, pp. 241–249, Mar. 2012.

[18] T. B. Song *et al.*, "Nanoscale joule heating and electromigration enhanced ripening of silver nanowire contacts," (in English), *ACS Nano*, vol. 8, no. 3, pp. 2804–2811, Mar. 2014.

[19] H. H. Khaligh and I. A. Goldthorpe, "Failure of silver nanowire transparent electrodes under current flow," (in English), *Nanoscale Res. Lett.*, vol. 8, May 16, 2013, Art. no. 235.

[20] D. Chen, F. Zhao, K. Tong, G. Saldanha, C. Liu, and Q. Pei, "Mitigation of electrical failure of silver nanowires under current flow and the application for long lifetime organic light-emitting diodes," *Adv. Electron. Mater.*, vol. 2, 2016, Art. no. 1600167.

[21] S. R. Das *et al.*, "Evidence of universal temperature scaling in self-heated percolating networks," (in English), *Nano Lett.*, vol. 16, no. 5, pp. 3130–3136, May 2016.

[22] K. Maize *et al.*, "Super-Joule heating in graphene and silver nanowire network," (in English), *Appl. Phys. Lett.*, vol. 106, no. 14, p. 143104, Apr. 6, 2015.

[23] P. Y. Huang *et al.*, "Grains and grain boundaries in single-layer graphene atomic patchwork quilts," (in English), *Nature*, vol. 469, no. 7330, pp. 389–392, Jan. 20, 2011.
[24] P. Nemes-Incze *et al.*, "Revealing the grain structure of graphene grown by chemical vapor deposition," (in English), *Appl. Phys. Lett.*, vol. 99, p. 023104, no. 2, Jul. 11, 2011.
[25] S. Kumar, N. Pimparkar, J. Y. Murthy, and M. A. Alam, "Theory of transfer characteristics of nanotube network transistors," (in English), *Appl. Phys. Lett.*, vol. 88, no. 12, p. 123505, Mar. 20, 2006.
[26] S. Kumar, N. Pimparkar, J. Y. Murthy, and M. A. Alam, "Self-consistent electrothermal analysis of nanotube network transistors," (in English), *J. Appl. Phys.*, vol. 109, no. 1, pp. 014315-1–014315-9, Jan. 1, 2011.
[27] M. P. Gupta, L. Chen, D. Estrada, A. Behnam, E. Pop, and S. Kumar, "Impact of thermal boundary conductances on power dissipation and electrical breakdown of carbon nanotube network transistors," (in English), *J. Appl. Phys.*, vol. 112, no. 12, p. 124506, Dec. 15, 2012.
[28] M. P. Gupta and S. Kumar, "Numerical study of electrical transport in co-percolative metal nanowire-graphene thin-films," *J. Appl. Phys.*, vol. 120, no. 17, p. 175106, 2016.
[29] S. Kumar, M. A. Alam, and J. Y. Murthy, "Effect of percolation on thermal transport in nanotube composites," *Appl. Phys. Lett.*, vol. 90, no. 10, p. 104105, 2007.
[30] J. H. Chen, C. Jang, S. D. Xiao, M. Ishigami, and M. S. Fuhrer, "Intrinsic and extrinsic performance limits of graphene devices on $SiO_2$," (in English), *Nature Nanotechnol.*, vol. 3, no. 4, pp. 206–209, Apr. 2008.
[31] A. T. Bellew, H. G. Manning, C. G. da Rocha, M. S. Ferreira, and J. J. Boland, "Resistance of single ag nanowire junctions and their role in the conductivity of nanowire networks," (in English), *ACS Nano*, vol. 9, no. 11, pp. 11422–11429, Nov. 2015.
[32] E. Pop, V. Varshney, and A. K. Roy, "Thermal properties of graphene: Fundamentals and applications," *MRS Bull.*, vol. 37, no. 12, pp. 1273–1281, 2012.
[33] Z. Cheng, L. Liu, S. Xu, M. Lu, and X. Wang, "Temperature dependence of electrical and thermal conduction in single silver nanowire," *Sci. Rep.*, vol. 5, 2015, Art. no. 10718.
[34] I. M. Abdulagatov, S. N. Emirov, T. A. Tsomaeva, K. A. Gairbekov, S. Y. Askerov, and N. A. Magomedova, "Thermal conductivity of fused quartz and quartz ceramic at high temperatures and high pressures," *J. Phys. Chem. Solids*, vol. 61, no. 5, pp. 779–787, May 1, 2000.
[35] Z. Chen, W. Jang, W. Bao, C. N. Lau, and C. Dames, "Thermal contact resistance between graphene and silicon dioxide," *Appl. Phys. Lett.*, vol. 95, no. 16, p. 161910, 2009.
[36] Q. K. Yu *et al.*, "Control and characterization of individual grains and grain boundaries in graphene grown by chemical vapour deposition," (in English), *Nature Mater.*, vol. 10, no. 6, pp. 443–449, Jun. 2011.

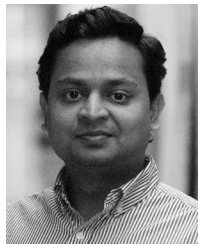

**Man Prakash Gupta** received the B.Tech. and M.Tech. degrees in mechanical engineering from IIT Kanpur, Kanpur, India, in 2009, and the Ph.D. degree in mechanical engineering from Georgia Institute of Technology, Atlanta, GA, USA, in 2014. He was a Postdoctoral Fellow in mechanical engineering with Georgia Institute of Technology from 2015 to 2016. He is currently a Research Engineer with Ford Motor Company, Dearborn, MI, USA His current research interests include electronics cooling and electrothermal modeling and simulation of electronic materials and devices for both low- and highpower applications. He received the Best Paper Award from the IEEE and the Best Poster Awards from ASME. He received the Sigma Xi Best Ph.D. Thesis Award at Georgia Institute of Technology in 2015.

**Nitish Kumar** received the B.Tech. degree in aerospace engineering from Indian Institute of Technology Kanpur, Kanpur, India, in 2012, and the M.S. degree in mechanical engineering from Purdue University, West Lafayette, IN, USA, in 2015. He is currently working toward the Ph.D. degree in mechanical engineering at Georgia Institute of Technology, Atlanta, GA, USA. His current research focuses on the electron and thermal transport in carbon nanotube network thin-film transistors and $Ga_2O_3$ devices.

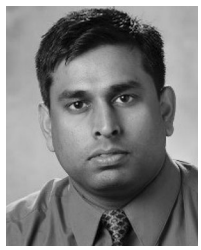

**Satish Kumar** received the Ph.D. degree in mechanical engineering and the M.S. degree in electrical and computer engineering from Purdue University, West Lafayette, IN, USA, in 2007. He is currently an Associate Professor with the George W. Woodruff School of Mechanical Engineering, Georgia Institute of Technology, Atlanta, GA, USA. He has authored or co-authored more than 100 journal or conference publications. He received the Purdue Research Foundation Fellowship in 2005, the Summer Faculty Fellowship from the Air Force Research Laboratories in 2012, the Woodruff School Teaching Fellowship in 2013, the DARPA Young Faculty Award in 2014, the Sigma Xi Young Faculty Award in 2014, and the Woodruff Faculty Fellow in 2017.